Creation of a Real-time Blood Chemistry Analyzer using In-Line Raman Resonance Spectroscopy

William D'Angelo, PhD, Jacob Glaser, MD, Senay Tewolde, PhD, Andrew Peitzsch, Justin Bequette, RN, Katie Geary, Robert Brothers, Ashley Dacy, PhD, April Cadena, Jacqueline-Rae Villaneuva

FINAL REPORT

Date: November 19, 2021

59th Medical Wing
Office of the Chief Scientist
1632 Nellis, BLDG. 5406
JBSA Lackland AFB, TX 78236-7517

DECLARATION OF INTEREST

The views expressed in this article are those of the authors and do not necessarily reflect the official policy or position of the Department of the Air Force, Department of Defense, nor the U.S. Government. This work was funded by Project Code Number AC12EM01. Authors are military service members, employees, or contractors of the US Government. This work was prepared as part of their official duties. Title 17 USC §105 provides that 'copyright protection under this title is not available for any work of the US Government.' Title 17 USC §101 defines a US Government work as a work prepared by a military service member, employee, or contractor of the US Government as part of that person's official duties.

NOTICE AND SIGNATURE PAGE

Using Government drawings, specifications, or other data included in this document for any purpose other than Government procurement does not in any way obligate the U.S. Government. The fact that the Government formulated or supplied the drawings, specifications, or other data does not license the holder or any other person or corporation or convey any rights or permission to manufacture, use, or sell any patented invention that may relate to them.

Qualified requestors may obtain copies of this report from the Defense Technical Information Center (DTIC) (http://www.dtic.mil).

CREATION OF A REAL-TIME BLOOD CHEMISTRY ANALYZER USING IN-LINE RAMAN RESONANCE SPECTRSCOPY

CHAGOY.EDWARD.A.1132159340
Digitally signed by CHAGOY.EDWARD.A.1132159340
Date: 2023.07.26 11:52:56 -05'00'

Edward Chagoy, DAF
Program Analyst
Trauma, Hemostasis & Resuscitation (AFT2R)
59MDW Office of the Chief Scientist

DEL MONACO.DIANA.V.1369906131
Digitally signed by DEL MONACO.DIANA.V.1369906131
Date: 2023.07.26 10:20:58 -05'00'

Diana del Monaco, Ph.D.
Acting Director, Trauma & Clinical Care
59MDW Office of the Chief Scientist

This report is published in the interest of scientific and technical information exchange, and its publication does not constitute the Government's approval or disapproval of its ideas or findings.

REPORT DOCUMENTATION PAGE

Form Approved
OMB No. 0704-0188

1. REPORT DATE	**2. REPORT TYPE**	**3. DATES COVERED**
19 November 2021	Final Report	08 DEC 17 – 31 DEC 19

4. TITLE AND SUBTITLE

Creation of a Real-time Blood Chemistry Analyzer using In-Line Raman Resonance Spectroscopy

5a. CONTRACT NUMBER

5b. GRANT NUMBER

5c. PROGRAM ELEMENT NUMBER

6. AUTHOR(S)
William D'Angelo, PhD, Jacob Glaser, MD, Senay Tewolde, PhD, Andrew Peitzsch, Justin Bequette, RN, Katie Geary, Robert Brothers, Ashley Dacy, PhD, April Cadena, Jacqueline-Rae Villaneuva

5d. PROJECT NUMBER
J917EM04

5e. TASK NUMBER

5f. WORK UNIT NUMBER
G1803COMM/DSN: 210-539-5334 (DSN:

7. PERFORMING ORGANIZATION NAME(S) AND ADDRESS(ES)
Naval Medical Research Unit San Antonio
3650 Chambers Pass, Building 3610
Fort Sam Houston, 78234

8. PERFORMING ORGANIZATION REPORT NUMBER

9. SPONSORING / MONITORING AGENCY NAME(S) AND ADDRESS(ES)
United States Air Force, 59th Medical Wing (59MDW/ST)
1255 Wilford Hall Loop, Building 4430
Lackland Air Force Base, 78236-9980

10. SPONSOR/MONITOR'S ACRONYM(S)
USAF 59th MDW/ST

11. SPONSOR/MONITOR'S REPORT NUMBER(S)

12. DISTRIBUTION / AVAILABILITY STATEMENT
Distribution A: Approved for public release; distribution is unlimited.

13. SUPPLEMENTARY NOTES

14. ABSTRACT-

In cases of extreme trauma, patients may be placed on extracorporeal life support or extracorporeal membrane oxygenation (ECMO). While on life support or ECMO, patients are closely monitored for hypothermia, acidosis, and coagulopathy – the so-called "trauma lethal triad". The current gold standard for measuring acidosis and other blood components is to test a small sample withdrawn from the patient using a blood gas analyzer. Blood analysis systems tend to be large, require perishable reagents and as such may not be feasible in limited environments or while treating a casualty en route. Here, we proposed a more compact method for analyzing blood components using Raman Resonance Spectroscopy (RRS) of whole blood within the ECMO circuit. The aims of the study were to (1) to identify the RRS signatures of hemoglobin-bound blood gases, lactate, and other metabolites in whole blood and (2) to develop the analysis tools to quantify the concentration of blood gas constituents based on the RRS measurements. The results of this study showed that peaks in the whole blood Raman spectra generally correlated with the measured levels of blood components. Additional data is required for the development of a neural network that could adequately characterize these spectra for use in medical monitoring.

15. SUBJECT TERMS- Extracorporeal Membrane Oxygenation, Raman Resonance Spectroscopy, Blood Chemistry, Machine Learning

16. SECURITY CLASSIFICATION OF:			**17. LIMITATION OF ABSTRACT:**	**18. NUMBER OF PAGES**	**19a. NAME OF RESPONSIBLE PERSON**
a. REPORT	**b. ABSTRACT**	**c. THIS PAGE**			Gerald T. Delong, CO, NAMRU-SA
U	U	U	UU	25	**19b. TELEPHONE NUMBER** *(include area code)* 210-539-5334 (DSN: 389-5334)

TABLE OF CONTENTS

1.0 EXECUTIVE SUMMARY

In cases of extreme trauma, patients may be placed on extracorporeal life support or extracorporeal membrane oxygenation (ECMO). While on life support or ECMO, patients are closely monitored for hypothermia, acidosis, and coagulopathy – the so-called "trauma lethal triad". The current gold standard for measuring acidosis and other blood components is to test a small sample withdrawn from the patient using a blood gas analyzer. Blood analysis systems tend to be large, require perishable reagents and as such may not be feasible in limited environments or when treating a casualty en route. Here, we proposed a more compact method for analyzing blood components using Raman Resonance Spectroscopy (RRS) of whole blood within the ECMO circuit. The aims of the study were to (1) to identify the RRS signatures of hemoglobin-bound blood gases, lactate, and other metabolites in whole blood and (2) to develop the analysis tools to quantify the concentration of blood gas constituents based on the RRS measurements. The results of this study showed that peaks in the whole blood Raman spectra generally correlated with the measured levels of blood components. Additional data is required for the development of a neural network that could adequately characterize these spectra for use in medical monitoring.

2.0 INTRODUCTION

In cases of extreme trauma, especially cases of damage to the lungs or cardiovascular system, patients may be put on extracorporeal life support or extracorporeal membrane oxygenation (ECMO).[1] This involves placing cannulas into large blood vessels, typically in the neck and groin, which pump blood out of the body and into a circuit that oxygenates the blood, absorbs carbon dioxide, and circulates the blood back into the body. This assists the respiratory system in oxygenating the blood and removing carbon dioxide while allowing the heart and lungs to rest and recover.

ECMO patients are at risk of succumbing to hypothermia, acidosis, or coagulopathy which are collectively known as the "Trauma Triad of Death" among care providers.[2] For this reason, these patients are constantly monitored for symptoms of any of the three facets of the triad. While the ECMO system does affect blood pH by removing carbon dioxide, its overall ability to balance a patient's blood pH is very limited.[3] Blood samples are taken from the patient regularly and are analyzed by a blood gas analyzer (BGA) device. However, these repetitive samples can account for up to 20% of total blood loss from some patients and can cause anemia.[4] While providing critical information, these BGA systems are not adequate for use in combat casualty and en route care situations as the equipment and reagents create significant bulk and the number of tests that can be completed are limited by the amount of reagents that can be carried and stored for extended times. Most reagents need to be stored at room temperature or refrigerated. An improved system for blood testing must offer capabilities similar to the existing tests while reducing the requirement for blood sampling and these material burdens.

Raman resonance spectroscopy (RRS) is a technique that uses the interaction between light and molecular structures to determine "chemical fingerprints" of compounds.[5] Using a laser, the bonds of chemicals can be made to absorb energy and be excited into different vibrational modes. The bonds then relax to their normal vibrational modes and release this energy in the form of scattered

light at frequencies different from the original laser. This difference in frequencies can be measured and forms a spectrum of shifted frequency peaks, known as Raman peaks. The resulting spectrum can be used to uniquely identify the material that generated it. Raman spectroscopy releases much less energy, in the form of the shifted Raman peaks, than is either transmitted through the material or is emitted through fluorescence. This means filtering and signal processing are required to extract useful quantitative information from the Raman spectrum.

Over the past four decades, Raman spectroscopy has been used to attempt to analyze blood and blood components in a variety of ways.[6] The main focus of prior research has been understanding the contribution of hemoglobin to the Raman signal, both in isolation and in red blood cells (RBCs). Hemoglobin makes up 95% of the dry weight of RBCs, which in turn make up approximately 40% of human whole blood. Hemoglobin is an extremely strong source of Raman scatter.[7] The hemoglobin signal inevitably dominates the signal in a Raman reading of blood and is an important consideration in the design of any blood-focused RRS study. Water is another large component of blood, but in contrast to hemoglobin, water is not a significant source of Raman scatter.[8] The properties of weak sources of scatter typically cause researchers to dehydrate water-based molecules on metallic surfaces to increase scattering properties thereby increasing signal strength. However, whole blood dehydration can cause denaturation bands to appear in the signal.[9] Previous work has attempted to analyze specific blood analytes, including glucose, by removing these spectral background signals.[10]

In this project, the objective was to develop a system that could measure blood components noninvasively and in real time via RRS analysis of whole blood as it circulated through the ECMO system. Measurements were taken through a quartz crystal chamber added in line with the ECMO tubing to act as an optical sampling port. A Thermo Fisher DXR2 SmartRaman benchtop system (Thermo Fisher Scientific, Waltham, MA) provided high quality measurements and the ability to optimize parameters. A small, portable Pendar Resonance Raman Spectroscopy system (Pendar Technologies, Cambridge, MA), developed to measure peripheral muscle oxygen saturation, was also investigated. The Pendar system is of a size that would be suitable for restrictive environments and en route care. Following collection of the RRS data, a fluorescence correction and signal processing algorithm were used to prepare the data for the training and testing of a novel machine learning algorithm with the purpose of detecting signals of importance for patient monitoring. This report outlines the methodologies for developing this system as well as initial test results and goals for further development.

3.0 METHODS, ASSUMPTIONS AND PROCEDURES

ECMO Circuit and Raman Measurements

Preliminary runs using the Raman system were conducted to collect baseline information on various components of the study. These scans were to help the research staff in selecting final parameters for the bulk of data collection. In establishing Raman parameters, factors were evaluated such as excitation wavelength, excitation duration, background readings and tubing material effects. Further trials were completed employing a complete ECMO circuit described below. All data from this phase of testing were collected using porcine whole blood and the SmartRaman system. Porcine whole blood was used to allow for more regular deliveries and in quantities that would meet the requirements for testing. The primary requirement being that 2 L

of blood was needed per experimental session to fill the custom ECMO circuit. The data collected was used to build a database of Raman spectra readings which were later corrected for fluorescence and flow-induced distortions using a custom built signal processing algorithm before serving as the training and testing data for machine learning.

The CARDIOHELP Portable ECMO System (Getinge Group, Sweden) was chosen because of its small size and ability to support en route care. A custom circulatory model was designed using medical grade tubing (Gentige Group, Sweden) to connect all necessary components of the ECMO and Raman imaging systems (Figure 1). Blood passed through the standard CARDIOHELP circuit to which two square quartz crystal cuvettes (G.M. Associates, Oakland, CA) were inserted. These optically transparent cuvettes were housed inside the Thermo Fisher SmartRaman sample analysis box and a custom-built analysis box for the Pendar RRS. After imaging, the blood returned to the reservoir via the circulatory tubing. The reservoir bag was used to add blood to the system at the beginning of testing and after doping. A Micro-Temp LT water bath heater (Cincinnati Sub-Zero Products LLC, Cincinnati, OH) was connected to the CARDIOHELP to control the blood temperature. Upon receipt of the porcine blood for each session, the blood was added to the circuit and allowed to run at a rate of 1-3 L/min for approximately 1 hour or until reaching 37° C, the average temperature of the human body.

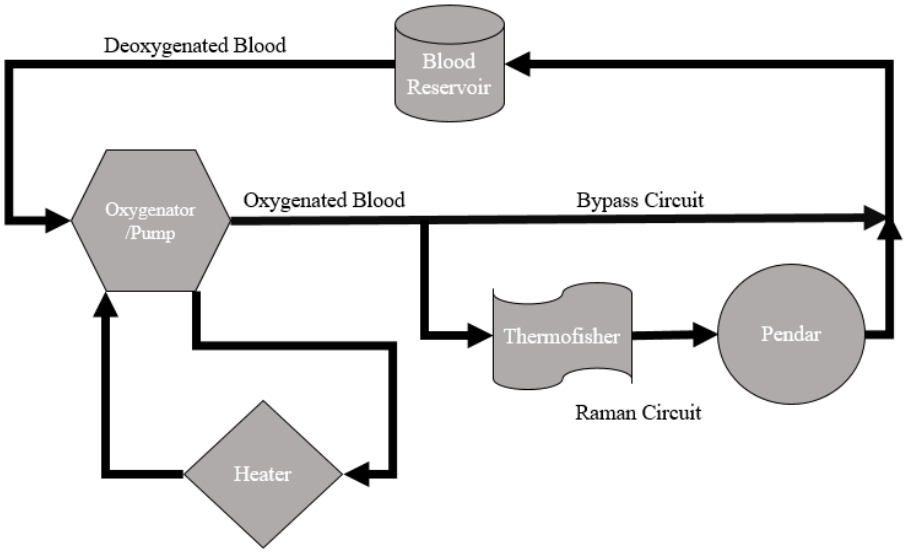

Figure 1. A schematic drawing of the oxygenation and Raman measurement circuit used to collect data during this study.

Upon reaching the proper temperature, the CARDIOHELP's pump mechanism was set to a flow rate of 3 L/min and allowed to circulate for five minutes to normalize before obtaining measurements from the SmartRaman and Pendar systems. The Pendar system was investigated to ensure that a Raman signal could be reliably measured and these spectra were not included in the analysis below. For the machine learning analysis, Raman measurements were all taken at 10 mW of power with a 532 nm laser using High-Resolution grating on the SmartRaman. Raman measurements were taken by averaging six exposures together to remove noise and cosmic ray interference. Fifteen-second exposures were used for the majority of training; additionally, five-second exposures were collected to determine if smaller exposures were adequate and yielded

similar measurements. The flowrate was then set to 1 L/min and given two minutes to normalize before collecting the SmartRaman data points. Finally, using surgical clamps, the circuit tubing before and after the Raman circuit were closed to reduce the flow rate to 0 L/min. After the collection of all baseline data, a 3 mL syringe was used to extract 2.5 mL of blood from the system via a port in the CARDIOHELP system for testing in the BGA. Using the same port, a 100 mL syringe was used to extract 100 mL of blood for the incorporation of the analyte to be doped.

For this study, blood glucose, creatinine, and lactate were the analytes of interest as well as the blood pH. During each session, key analytes or combinations of analytes were studied to determine the effect of their increased concentration on the Raman spectra. A complete list of the analyte combinations can be seen in Table 1. A Radiometer ABL 800 BGA (Radiometer Medical ApS, Denmark) was used to determine control concentrations of these components. The value of each analyte's concentration was obtained from the ABL 800 BGA for use in calculations to determine the amount of analyte required to bring the concentration in the blood to those specified in Table 1. Note that the concentrations were set to high levels to attempt to provide distinct Raman peaks but were below those that would cause hemolysis. The initial test was repeated twice (trials 1 and 2 with glucose at 1.5 g/dL) to compare to each other for establishing consistency in the procedure.

Trial Number	1	2	3	4	5	6	7	8	9	10	11	12
Analyte	G	G	LA	C	LA + G	G + C	C + LA	LA + G	G + C	C + LA	C + LA + G	C + LA + G
Target Concentration	1.5 g/dL	1.5 g/dL	pH 6.5	3 mg/dL	pH 6.5 – 1.5 g/dL	750 mg/dL – 2 mg/dL	1.5 mg/dL – pH 6.5	pH 6.5 – 750 mg/dL	750 mg/dL – 2 mg/dL	1.5 mg/dL – pH 6.5	1.5 mg/dL – pH 6.5 – 750 mg/dL	1.5 mg/dL – pH 6.7 – 750 mg/dL

Table 1. Analyte concentration and pH targets for Creatinine (C), Glucose (G) and Lactic Acid (LA).

The doping dose was incorporated and mixed using a second 100 mL syringe connected using a female/female adapter to the 100 mL syringe containing the blood drawn from the reservoir bag. The 100 mL of doped blood was added back into the system again via the reservoir bag. The system was then allowed to mix for approximately 5-10 minutes at a rate of 3 L/min before the Raman and BGA measurements reoccurred. For each session, the cycle was completed 4 times with the blood being doped at least twice and the first and last measurements being used to establish baseline and final analyte levels.

Fluorescence correction

Fluorescence correction, flow correction, and feature selection were all handled in the R statistical computing language (R Core Team, Institute for Statistics and Mathematics, Wirtschaftsuniversität, Vienna, Austria) using the RStudio environment (RStudio PBC., Boston,

MA). Fluorescence and flow correction were handled by functions created as part of a file containing a collection of helper functions collectively called *SpectralPreprocessing*. A flow diagram depicting the function of the *SpectralPreprocessing* helper files can be found below in Figure 2. This multi-step correction process was critical to prepare the data before it was analyzed by the machine learning algorithm. By putting all data through the same processes, it insured that the format of each piece of data that passed through the algorithm was as similar as possible to aid the algorithm in detecting patterns and to improve the overall fit for each signal processing method. This correction process also allows distinctive qualities of each of the groups (flow, exposure, and analyte) to become more prominent.

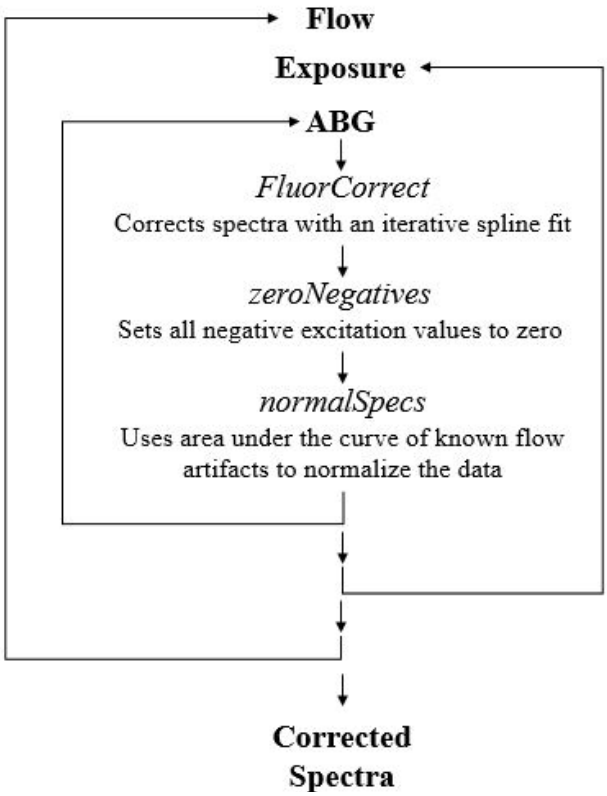

Figure 2. Flow diagram depicting the multiple steps and feedback loops performed in "SpectralPreprocessing" to properly prepare the data to be fed into the machine learning algorithm.

The bulk of the main code is housed within 5 conditional feedback loops: one for the flow rates (0 L/min, 1 L/min, and 3 L/min), one for the exposure times (5 sec, 15 sec), one for the analytes (glucose, lactose, creatinine, and pH), one for the padding value search (values from 0 to 200), and finally one for the number of spline points (values from 3 to 50). The first process to be completed within these loops is to preprocess the data by calling functions from the *SpectralPreprocessing* file. The first function called is the *fluorCorrect* function which takes in the spectra, the type of correction to be performed (spline), and the number of spline points being evaluated in the current round of the loop. This function triggers a series of subfunctions within the *SpectralPreprocessing* library. The first of the subfunctions identifies the local minima in each region of the spectroscopy data, and the coordinating wavelength. A spline curve is then fit to these minima, which can then be subtracted from the actual excitation values of the spectra.

Once the curves are subtracted, the resulting spectra are processed through the *zeroNegatives* function. The *zeroNegatives* function takes in the spectra returned by the *fluorCorrect* function. This step locates all spectra values that are less than zero, and sets them to zero so there are no negatives in the dataset. These negative points are created when the spline curve occasionally is of a higher intensity than the true values of the spectra. While the spline is being fit to the local minima, the raw spectrogram may not increase at the rate set by the curve between two minima values. A negative spectra value does not naturally occur and therefore would interfere with the processing of the data in later steps. The function returns the zeroed spectra which can then pass through the remaining preprocessing steps.

The final step in the correction process is the *normalSpecs* function which, like the *fluorCorrect* function, triggers a series of subfunctions to complete its task of normalizing the data. Flow correction is handled by normalizing the spectra based on hemoglobin values as well as features in the blood not associated with the analytes being studied. The *normalSpecs* function input includes the zeroed spectra from the previous step as well as a vector of the hemoglobin values for the sample. Prior to beginning the analysis, key wavenumbers that were indicative of flow disturbances during the preliminary tests were identified. The area under the curve at each of these identified disturbance wavenumbers was calculated as well as the hemoglobin ratio of area to width and hemoglobin levels. This information was then used to fit the data with yet another spline curve which was then used as a normalization factor to be multiplied by the spectra from the *fluorCorrect* output.

Following the correction process, the number of data points was reduced to concentrate the algorithm on the peaks of interest. A function called *selectKeyPoints* was created to accept the corrected spectra from the above process as well as a vector of "key points" to concentrate the data around. The purpose of this was to reduce the overall number of points passing through the machine learning algorithm. In turn, this would reduce the processor time spent training for these preliminary parameter searches while still preserving all relevant information. The vector of key points used in this algorithm was held constant for all values in the five conditional loops. The values in this vector represent key points identified in the preliminary testing.

Machine learning

Machine learning is a rapidly evolving and highly adaptable technology with several commonly used methods for processing linear signals. The code developed for this portion of the study is similar to the *HyperParameter Tuning* function developed by Amazon Web Services' (AWS) Amazon SageMaker (Amazon.com, Seattle, WA). As with the *HyperParameter Tuning* function, the code developed here cycled through a list of potential parameter values comparing root mean square error (RMSE) values of test data to determine the optimal algorithm. However, differing from the AWS function, this code also cycled through a series of pre-selected linear signal processing methods to determine the optimal algorithm.

The methods evaluated in this study include: principal component regression (PCR), partial least squares (PLS), and support vector regression which comes in two forms of functional kernels, linear (SVR-L) and Gaussian radial (SVR-R). All of these methods involve fitting a multidimensional line between independent input variables and predicted resultant dependent variables with minimal error.[11-14] PCR identifies principal components that describe the variation

between samples, using these to model and predict unknown samples. PLS is similar to PCR but selects for components that both describe the data and correlate highly to the outcome differences. SVR attempts to transform the data such that a high dimensional function of the input data to the outcome data can be found with minimum error, and uses different kernels to reshape the line to account for non-linearities. These methods go about this prediction and model adjustment in different ways, and thus may yield different predictive performance from each other. PLS and SVR are supervised methods that helps target the model towards explaining the outcome, but this may overfit on noise that isn't truly varying in the signal. SVR requires higher levels of computation compared to PCR and PLS due to its high dimensionality. All three methods were considered to determine which combination of signal processor, padding values, and spline points would best fit the data.

All machine learning was conducted in the R statistical computing language using the RStudio environment and the Classification and Regression Training (CARET) package (Max Kuhn, https://topepo.github.io/caret/). The algorithm was designed to accept data in groupings distinguished by flow rate and exposure duration to prevent the introduction of variation that could lead to potential misfitting in the model. As such, training and testing code were nested inside five "for loops": one for flow rate (0, 1, 3 L), one for exposure time (5, 15 seconds), one for analyte (creatinine, glucose, lactic acid, pH), one for potential padding values (0 – 200), and one for potential spline points (3 – 50). Upon accessing each subset of data the algorithm preprocesses the data with the functions in the *SpectralPreprocessing* library before separating the data into the standard 80:20 ratio of training-to-testing samples. For the current dataset this yielded 20 training data points and 5 testing data points. A flow diagram of the algorithm can be found in Figure 3.

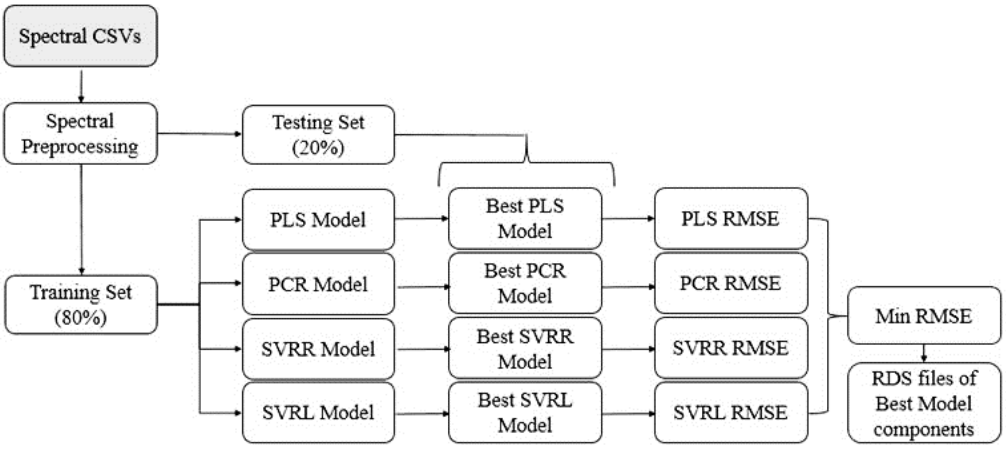

Figure 3. A flow diagram displaying the overall process created by the code to generate machine learning algorithms (see text for a full description) and determine their root mean square error (RMSE) in fitting the dataset. The input is comma separated value (CSV) files and the output is R data serialized (RDS) files.

Upon establishing the training group, the data in this subset from each combination of flow rate, exposure time and analyte of focus were used to train an algorithm using each signal processing method, each padding value, and each spline point value. This resulted in the generation of 4,608 different algorithms. A diagram of the code's structure can be seen in Figure 3. The code was then

able to detect which algorithm was most successful by means of tracking the root mean square error (RMSE) for each algorithm when tested with the data in the test set established earlier. This yielded 24 final algorithms that were deemed the best fit for their respective flow rates, exposure times, and analytes. The code then saved all weights, parameters, and outputs of the best algorithms and kept a tally of which padding values and spline point values most often lead to the most successful algorithms.

4.0 MAJOR EVENTS/MILESTONES/SUCCESS

- Kick-Off Meeting – 02/2018
- Abstract submission for 29th Annual ELSO conference – 07/2018
- Poster presentation – 29th Annual ELSO Conference, 09/2018
- Initiate and begin Raman-ECMO apparatus development – 02/2019
- Begin testing of Raman-ECMO apparatus – 05/2019
- Procurement of equipment and supplies complete - 01/2020
- Data collection completed – 03/2020
- Data analysis complete – 04/2021
- Manuscript complete – 11/2021

5.0 RISK ASSESSMENT

5.1 Risk Analysis:

This project was initially assessed as low risk. Raman analysis of whole blood had not been performed in this manner previously, however, no major technical impediments were expected. Developing a machine learning algorithm was also novel to the effort with collecting a large enough sample size being an expected issue common to algorithm development.

5.2 Technical Challenges

For this initial study, a circuit had to be devised that could allow accurate ECMO flow rates and functionality while at the same time allowing a clean, repeatable Raman signal to be collected and allowing the ability to modify the levels of the analytes being studied. The result was that the circuit required on the order of 2 L of whole blood to operate. Sources of 2 L of fresh, whole blood are limited, expensive and did not offer the ability to control the baseline levels of the blood analytes. The accuracy of the analyte concentration "ground truth" for comparison to the Raman spectra and training of the network was dependent on the ABL800 BGA readings. With the swine whole blood samples, values well out of the typical physiological range were common. The effect of the accuracy of the calibration when far out of the expected range is unknown. While determining the RRS parameters, it was found that the power and duration of the laser exposure of the blood had to be balanced between obtaining a clean spectrum and maintaining blood cell viability. In order to address the apparent complexity of the Raman signal measured from whole blood,[7-9] machine learning algorithms were utilized to analyze the spectra. While this is a novel and powerful approach, machine learning still requires a well-characterized, repeatable signal and sufficient data with which to train the networks. In this study, with a focus on obtaining

optimized RRS signals, insufficient data was available with this system to fully exploit the machine learning technique.

6.0 TRANSITION PLAN

6.1 Military Relevance

Management of hemorrhage continues to be a top priority within military medicine.[15] While resuscitation protocols exist that reduce the pathology associated with hemorrhage, including the administration of blood and/or plasma, coagulopathy management and the use of tourniquets, a real-time tissue diagnostic platform capable of discriminating oxygenation/deoxygenation, and the presence of blood analytes associated with ischemic injury is essential. Hemorrhage induced by trauma can lead to loss of limbs, organ failure, and death.[16] Raman spectroscopy is a possible platform for a real-time diagnostic tool to characterize blood oxygenation and acidity. This tool would make it possible to have a durable, field-deployable, point-of-care analyzer, allowing critical information about blood constituents to be obtained both at the point of injury and across the entire spectrum of care. Within the scope of the completed works, the short term goal was to determine the feasibility of applying RRS techniques to analyze whole blood, including the employment of machine learning. The long-term goal of this project is to investigate the accuracy and efficacy of an in-line, real-time, RRS diagnostic platform in the field, for use to forecast the severity of shock and ischemia.

6.2 Transition Strategy

Raman resonance spectroscopy has the potential to become a vital medical monitoring technique. In order to transition this into a working medical device, further work would need to be completed to further explore the technical challenges of analyzing whole blood with RRS, for example, the mechanisms of the blood's interactions with the laser, and to collect additional data to train the machine learning algorithm. Once the algorithm is trained and shows satisfactory results using benchtop controls, testing in animals would be required to make verify accuracy and support safety in humans. Finally, testing and training would need to occur to adapt the algorithm to analyze human data. This algorithm would require review by the FDA under the "software as a medical device" regulations. At this point, commercialization would occur through the licensing of the technology to a medical device partner.

7.0 RESULTS

ECMO Circuit and Raman Measurements

Twenty five spectra were collected for each combination of flow rate and exposure period. In each of these spectral measurements, the peaks corresponding to each of the blood components were determined. Corresponding samples were passed through the ABL 800 BGA to record the calibrated values for comparison. Physiological normal values for swine and the range of observed values obtained from the ABL 800 can be found in Table 2.

	Physiological Normal		Observed	
	Minimum	Maximum	Minimum	Maximum
Creatinine (dg/L)	0.930	1.170	0.870	2.230
Glucose (mmol/L)	5.500	6.700	2.200	22.900
Lactic Acid (mmol/L)	0.500	5.500	5.700	18.000
pH	7.400	7.430	6.899	7.983

Table 2. Comparison of normal swine physiological levels for creatinine[17], glucose[17], lactic acid[18] and pH[19] and the range of observed values for each.

The observed creatinine and glucose measurements were typically within the normal to high physiological range. Lactate concentrations were all above normal physiological range. Observed blood pH measurements encompassed the entirety of the physiological range, as well as both above and below. Because samples did not often contain low normal and below normal values, the dataset is skewed. This also hampered manipulation of blood sample concentrations as analytes could only be added and not removed. Due to technical issues with the ABL 800, the first four blood gas measurements did not produce creatinine measurements and were not included for creatinine model training. As such, creatinine training had a train group size of 17 and a test group size of 4.

Fluorescence correction

Fluorescence correction removed most inter-run variation and brought all spectra within the same range (Figure 4). However, the corrected spectra still showed unaccounted for variation in the height of peaks. Flow rate correction was able to reduce this variation as shown in Figure 5.

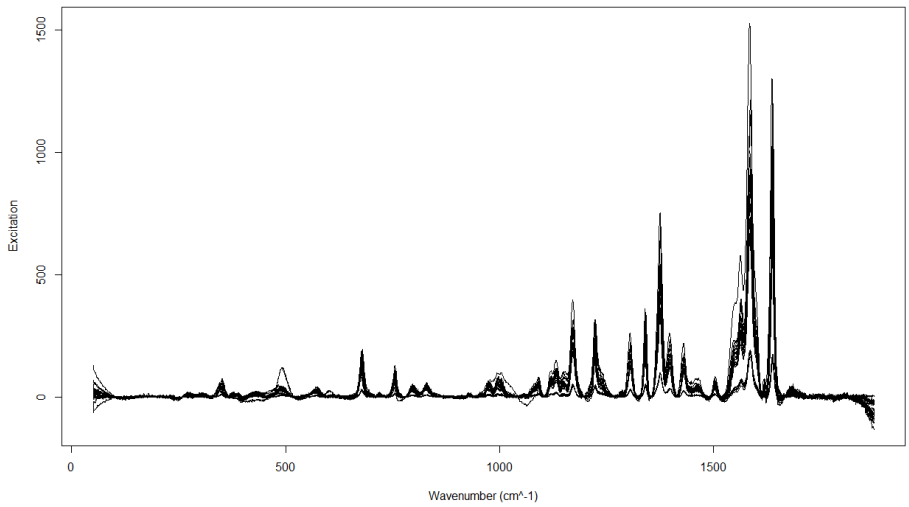

Figure 4. Fluorescence corrected Raman spectra of blood flowed at 3 L/min with a 15 second exposure.

This suggests that the spectra are normalized to a level where the remaining variation in signal should be due to changes in the concentrations of blood components. This correction was effective for all spectra, as illustrated by spectra collected at a flow rate of 3 L/min with a 15-second exposure.

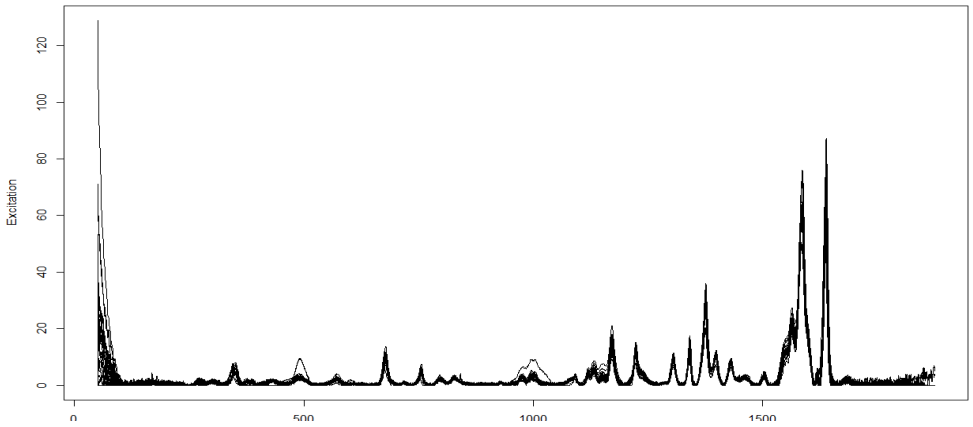

Figure 5. Fluorescence and flow corrected Raman spectra of blood flowed at 3 L/min with a 15 second exposure.

Machine Learning

The initial analysis code processed all flow rates, exposure times, analytes, padding values and spline point values. The output from this code was a collection of R data serialized (RDS) files containing the parameters, errors, and other critical information about the "best" algorithm for each combination of flow rates, exposure times, and analyte, as determined by the algorithm with the number of spline points and padding that resulted in the minimum RMSE value. From this data, the optimal algorithm type, padding, and spline points could be identified to yield the lowest RMSE for the detection of each analyte. Table 3 details the best signal processing method and final RMSE for each combination of flow rate, exposure time and analyte.

For measuring pH levels, PCR was found to be the best model at both 5 and 15 second exposure times at 0 L/min, as well as at 15 seconds at a flow rate of 1 L/min. Support vector machines were also successful in measuring pH with SVR-L being the best fit for 15 seconds of exposure at 1 L/min, and SVR-R being the best fit for 5 seconds of exposure at 1 L/min and 3 L/min. The variation in RMSE values amongst all of the top models for pH at any flow rate and exposure combination was relatively tight, ranging from 0.22 to 0.48. This error range was the smallest of any of the analytes and approaching the range that could be suitable for medical monitoring.

Creatinine predictors varied between SVR-Ls, PCR, and PLS. PLS was the identified strategy for predicting creatinine at 5 seconds of exposure for static flow, and 15 seconds of exposure for 3 L/min of flow. The linear support vector machines were identified at both 5 and 15 seconds for 1 L/min and 5 seconds of exposure for 3 L/min. PCR was identified for 15 seconds of exposure at both 0 and 3 L/min. The RMSE values for creatinine ranged from 0.39 to 0.57. This range was both narrow and approaching the range that could be tolerable for medical monitoring.

Support vector machines were superior in nearly every combination of flow rate and exposure time for detecting glucose. An SVR-L was found to be best for measuring glucose at 5 seconds of exposure at 0 L/min and 3 L/min, as well as at 15 seconds of exposure for 3 L/min. An SVR-R was superior for detecting glucose at 15 seconds exposure at 0 L/min and 5 seconds exposure at 1 L/min. PLS was identified as the superior method for detecting glucose at 15 seconds exposure during flows of 1 L/min. However, the RMSE values for all six of these predictors ranged from 5.8 to 8.15 which is far outside the acceptable error for potential use in medical monitoring.

0 L/min								
Exposure (s)	**5**				**15**			
Analyte	**pH**	**Glu**	**Lac**	**Crea**	**pH**	**Glu**	**Lac**	**Crea**
Method	PCR	SVR-L	SVR-R	PLS	PCR	SVR-R	SVR-R	PCR
RMSE	0.30891	6.71186	3.11714	0.46419	0.33869	5.8122	3.41623	0.39854
1 L/min								
Exposure (s)	**5**				**15**			
Analyte	**pH**	**Glu**	**Lac**	**Crea**	**pH**	**Glu**	**Lac**	**Crea**
Method	SVR-R	SVR-R	SVR-L	SVR-L	SVR-L	PLS	SVR-L	SVR-L
RMSE	0.246705	6.48214	3.62042	0.57228	0.47749	5.92106	3.29991	0.4334
3 L/min								
Exposure (s)	**5**				**15**			
Analyte	**pH**	**Glu**	**Lac**	**Crea**	**pH**	**Glu**	**Lac**	**Crea**
Method	SVR-R	SVR-L	SVR-R	SVR-L	PCR	SVR-L	SVR-L	PLS
RMSE	0.22445	8.14742	3.69595	0.38703	0.28106	8.40011	3.08061	0.39279

Table 3. The optimal signal processing methods and root mean square error (RMSE) values for all analytes at each combination of flow rate and exposure time. PCR: Principle component regression; SVR-L: support vector regression, linear; SVR-R: support vector regression, Gaussian radial; PLS: partial least squares.

Similar to glucose, support vector machines were identified as the ideal predictor for identifying lactose under every combination of exposure and flow. Linear kernels were superior for 5 and 15 second exposures for flows of 1 L/min, as well as 15 seconds of exposure at 3 L/min. Radial kernels were identified as the superior for all remaining combinations. RMSE value for the lactose predictors ranged from 3.08 to 3.70, a tighter range than the glucose predictors, but still largely above the tolerable error for potential use in medical monitoring.

Looking further into the ability of machine learning algorithm to detect creatinine, a plot of the training and testing data compared to the algorithm's prediction line can be seen in Figure 6. Each of these groupings of plots represents the algorithm's success for the three flow rates that were studied. It appears that as the flow rate increases, the measurements become increasingly more uniform and linear. While insufficient evidence exists to support this conclusion at this time, it should be further examined to determine why increased flow rate returns a more uniform measurement.

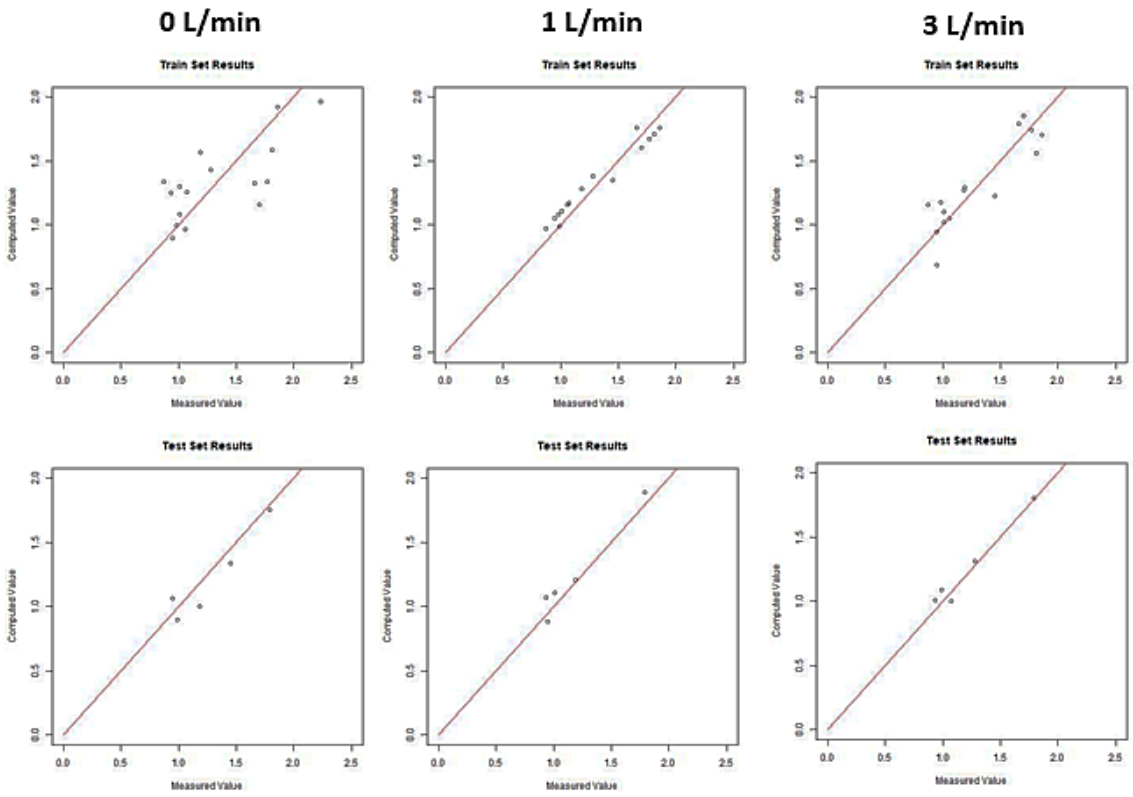

Figure 6. Plots of the training and test data and resulting model for 15 seconds exposure time focusing on creatinine at flow rates of 0 L/min (static), 1 L/min, and 3 L/min.

As the code ran through all five conditional loops, a counter was used to keep track of the number of times each value of spline points and padding, respectively, were used in the model identified as the "best fit." At the conclusion of the processing steps, the most frequently identified number of spline points was 35 and the padding value was 125. Using this information, the code was run a second time with the conditional loops for spline points and padding values replaced with each of these respective values. The results of this code outputted a data sheet with the information for four algorithms, one for each of the four linear signal processing methods (PCR, PLS, SVRL-L, and SVR-R). These output files were then used to construct a table for use in comparing the RMSE values between algorithms with the same signal processing method, flow rate, exposure time, and analyte to better understand the relationships between these factors (Table 4).

	Creatinine						Glucose					
	0 L/min		1 L/min		3 L/min		0 L/min		1 L/min		3 L/min	
	5 s	15 s	5 s	15 s	5 s	15 s	5 s	15 s	5 s	15 s	5 s	15 s
PCR	0.392	0.362	0.376	0.429	0.384	0.318	4.951	4.047	4.414	5.641	5.565	5.487
PLS	0.337	0.398	0.376	0.334	0.296	0.274	5.342	4.933	4.071	4.829	5.438	4.584
SVR-L	0.356	0.338	0.374	0.314	0.327	0.297	5.299	4.884	4.056	4.213	5.369	6.192
SVR-R	0.398	0.299	0.381	0.329	0.306	0.329	5.491	4.067	3.883	5.924	4.385	0.126

	Lactose						pH					
	0 L/min		1 L/min		3 L/min		0 L/min		1 L/min		3 L/min	
	5 s	15 s	5 s	15 s	5 s	15 s	5 s	15 s	5 s	15 s	5 s	15 s
PCR	3.403	3.223	2.985	2.327	3.695	3.114	0.288	0.284	0.284	0.252	0.268	0.250
PLS	3.099	3.461	2.934	2.859	3.344	3.304	0.346	0.356	0.248	0.203	0.228	0.203
SVR-L	3.456	3.341	3.116	3.257	3.608	4.044	0.330	0.327	0.251	0.209	0.238	0.201
SVR-R	3.308	2.866	3.052	2.603	3.492	2.876	0.172	0.240	0.246	0.185	0.195	0.202

Table 4. RMSE values of all algorithms generated for each combination of flow rate, exposure time, and analyte using each of the 4 signal processing methods at padding = 125 and spline points = 35.

From this data, trends were observed for the relationships between the RMSE values of each algorithm. RMSE values are fairly close for all four signal processing methods; either all four methods performed well, or all performed poorly for the given analyte, flow rate, and exposure time. The algorithms generated were more accurate for predicting creatinine and pH than they were for glucose and lactose.

8.0 CONCLUSION/DISCUSSION

ECMO Circuit and Raman Measurements

Overall, the ECMO circuit constructed for the in-line RRS measurements successfully allowed the real-time gathering of whole blood spectra. There were a number of lessons learned with the initial approach described here. Background scans used to normalize the spectra would typically be collected every thirty minutes. In this study, this was not possible as the ECMO tubing passed directly through the Raman system and could not be removed when filled with blood for a session. Ambient temperature can affect Raman systems, and while the experiments were conducted in a small, climate controlled room, additional background scans could have reduced a potential source of error. The full effect of background scanning will need to be addressed with any future Raman field device. However, there are currently handheld systems that have overcome this limitation for field use. Examples include the Cora 100 (Anton Paar, GmbH, Graz, Austria) and the NanoRam (B&W Tek, LLC, Plainsboro, NJ) to name a few. A few pilot measurements were successfully collected with the Pendar device showing promise for a portable system.

A limiting factor in optimizing both the RRS system and the machine learning algorithm was the small number of samples that were collected because of the required blood volume and expense of running a complete ECMO circuit during each session. Each shipment of blood came from a different porcine specimen or multiple specimens with different delivery times and conditions. The

starting levels of each analyte in the blood shipments showed a very large degree of variation. Close monitoring and control of donor animal health, nutrition and hydration would be required to make these values less variable. For example, dehydration prior to the blood draw is a potential source of the high initial levels of lactic acid. Additional sample opportunities would have allowed more in depth examination of single analytes and the effects of the laser exposure (wavelength, power and duration) on the blood cells. As mentioned previously, analytes could only be added to the blood samples, not removed thus limiting the range of minimum values studied.

The viability of the blood cells and the proportions of cells that were lysed during key steps was not assessed. A potential for hemolysis occurred during the doping process when 100 mL of blood was removed from the system for the addition of the analyte(s). According to Fisher Clinical Services, when using a syringe it is critical to apply the proper speed and pressure to prevent cell wall shearing.[20] The doping of blood samples at the highest analyte concentrations was designed to approach hemolysis levels. These doping samples were required to be in quantities large enough to set the concentration of the entire ECMO circuit containing 2 L of blood, yet were initially added to only 100 mL of blood for mixing. On occasion, the blood inside of the 100 mL mixing syringe was noted to turn from red to brown, signaling potential damage to blood cells.

Normal flow rates for an adult human fully reliant on an ECMO system fall in the range of 4-6 L/min for maintaining oxygen delivery and CO^2 removal.[21] Flows in the "weaning" range (1.5-3 L/min) are supplemented by the patient's own organs regaining function.[22] The flow rates tested here fall more in line with weaning flow rates, but without a patient's organs in the loop to deliver oxygen and remove CO^2, the system employed here is appropriate for a proof of concept study to examine the effect of flow. Measurements at 5 L/min were attempted during early rounds of testing, but the CARDIOHELP system struggled with cavitation when approaching flowrates above 3.5 L/min. The cavitation or "chugging" is thought to be caused when the venous-side pressure is too low causing erratic flow or there is clotting in the arterial lines. [23] In practice, the system would not have the reservoir bag which may have also been a contributor.

Fluorescence Correction

The fluorescence correction algorithm developed for this study was a strong start, but needs continued development before the total package could reach a diagnostic and marketable level. One area of required further work would be to determine a more accurate measure of the flow rate in front of the spectrometer during spectrometry measurement. The more accurate the flow rate entered into the correction calculation is, the more accurate the overall spectral preprocessing correction can be. Once the corrections for flow rate are tuned, it is hopeful that the success of both the 5 and 15 second exposure period data will rise. As the algorithm is able to identify key features and patterns in the 15 second exposure period, which has already shown promise, it is hopeful that the algorithm can adapt to detect the same things from the shorter exposure period data using the transfer learning principle.

Machine Learning

Multiple forms of analysis were completed on the output of the code to determine optimal parameters for the detection of analytes separately and collectively, and to better understand the relationships between the flow rates, exposure times, and analytes based on their effect on the overall RMSE of the algorithms. The results of each branch of investigation allow for a better

understanding of how the network is operating, the types of patterns being detected and highlight potential areas of over fitting which would lead to a less adaptive algorithm. Using this information, further research could be guided to create a very powerful algorithm capable of identifying one or all potential analytes with a high level of accuracy and with built in safeguards to avoid overfitting.

A series of plots were generated in R to map the generated model against its corresponding testing and training data sets (Figure 4). The data shows a trend of both the test and training sets becoming more uniform and linear as the flow rate increases, yet the accuracy for predicting constituents was relatively poor. While multiple potential explanations arise, further work needs to be done to explain this finding.

The overall trends in RMSE values appeared to show a high potential to predict creatinine and pH and relatively poor potential to predict glucose and lactose. However, it is difficult to put these values into perspective without an appropriate comparison from the ABL 800 BGA. Data was sought from the ABL 800 BGA's manual and 510k submission.[24,25] Precision and accuracy numbers were presented in the form of an acceptable threshold for data based on the 95% confidence interval, which would not make for an easy comparison to RMSE. These numbers were reported for glucose, lactic acid, and pH, but no data was provided for creatinine. There was, however, information relaying that creatinine did have a slight interference (<1%) from both lactic acid and glucose. In a separate study analyzing the performance of the ABL 800 BGA against other BGA devices in the detection of creatinine, the ABL 800 BGA was reported to have a standard deviation of 0.6 umol/L in samples with an average concentration of 29 umol/L.[26] Neither of these values led to an appropriate value for comparison, and RMSE errors of controlled measurements from the ABL 800 BGA were unable to be collected.

While comparison values were unavailable, the RMSE values for glucose and lactose were so high that it is likely whatever the normal ABL 800 accuracy is, these numbers are above it. It is entirely possible this is because these analytes simply do not follow a linear path. Future code should be developed to attempt to fit the data with other signal processing methods, including potential algorithms for non-linear data.

From the results of running the code multiple times, it is shown that the models are much better at designing predictive algorithms for each analyte separately, and further fine tuning would be required to create a large predictive model capable of properly handling each of the four analytes. However, though the predictive models for separate analytes were more accurate than the overarching model, these algorithms were still inferior in accuracy to the BGA technique. With further fine tuning of the individual models and further data points, it is likely the accuracy could be increased to reach BGA levels.

The better performance of the increased exposure period (15 seconds) over the shorter exposure period (5 seconds) suggests that the longer laser exposure may not be damaging the flowing blood and allowing a better signal-to-noise ratio. However, insufficient data was collected to support this hypothesis statistically. Additional research needs to be conducted into a range of exposure periods to track the optimum exposure period to increase signal-to-noise ratio while ensuring the cells are not damaged by the laser. Additionally, more detailed research into the optimum wavelength

should be conducted before completing additional studies. A 532 nm wavelength was chosen for the purposes of this study as prior studies into the spectra of dried blood have shown promising results at wavelengths of 532 nm, 738 nm, and 830 nm.[27,28,10] Most previous work has been conducted with dried blood and dried plasma, and it is important to collect more baseline information on the effects of wavelength and exposure on *liquid* whole blood during both static and dynamic flow rates.

The results have shown that for some analytes, such as glucose, accurate models can be made. While these models do not yet provide the accuracy of the BGA technique, which is considered to be the gold standard, future work would hopefully reduce the error until the methods are comparable. This bodes well for the prospect of continuous and less invasive monitoring of critical patients using ECMO. These models were not transferable to shorter exposure duration data. An additional hope for future work would be to combine all these tests into one predictive model. This could improve computation time and storage space, and would likely make the system easier to use.

8.1 Future research directions

In extreme trauma cases where extracorporeal membrane oxygenation (ECMO) is necessary, standard blood assays may not provide up-to-date information on patient status and may lead to incorrect care decisions.[29] The present study demonstrated initial success with a novel system to monitor blood constituents and characteristics using a real-time, nondestructive, inline RRS system. With this initial success using a full ECMO system, future studies would benefit from using an ECMO simulator in order decrease the required blood volume and increase the data output. Further research into the fundamentals of measuring whole blood with the RRS would include a better understanding of the vitality of cells after laser exposure and a better quantification of the effect of flow rate. An additional focus could be on collecting more spectra to improve fluorescence correction and normalization methods. Other machine learning technologies such as neural networks should be explored.

A potential future direction for this project would be to combine it with near infrared spectroscopy (NIRS), which is another optical method that detects the energy of bonds in molecules. While Raman spectroscopy works by determining the energy emitted from an excited bond, NIRS works by passing through various frequencies of infrared light and detecting which frequencies are absorbed. Because of this different detection method, chemicals that may not emit Raman excitation may be detectable with NIRS. A combination system could expand the range of non-invasive sensing, as well as providing two measurements that can be compared against each other to better improve detection accuracy.

9.0 DELIVERABLES

9.1 Publications:

1. Final Technical Report, Defense Technical Information Center

9.2 Presentations:

1. Poster presentation – 29th Annual ELSO Conference, 09/2018

10.0 COST

1. FY17: Planned $500,000; Received $500,000; Obligated $500,000; Expended $494,868.68

2. FY18: Planned $500,000; Received $500,000; Obligated $492,000; Expended $492,000

3. Total: Planned $1,000,000; Received $1,000,000; Obligated $992,000; Expended $986,868.68

11.0 REFERENCES

1. Cordell-Smith J, Roberts N, Peek G, Firmin R. Traumatic lung injury treated by extracorporeal membrane oxygenation (ECMO). ScienceDirect. https://doi.org/10.1016/j.injury.2005.03.027. Published 2020.
2. Mitra B, Cameron P, Parr M, Phillips L. Recombinant factor VIIa in trauma patients with the 'triad of death'. ScienceDirect. https://doi.org/10.1016/j.injury.2011.01.033. Published 2020.
3. Melania M. Bembea R. Magnitude of Arterial Carbon Dioxide Change at Initiation of Extracorporeal Membrane Oxygenation Support Is Associated with Survival. PubMed Central (PMC). https://www.ncbi.nlm.nih.gov/pmc/articles/PMC4557460/. Published 2020.
4. Barie P. Phlebotomy in the intensive care unit: strategies for blood conservation. Critical Care. 2004;8(Suppl 2):S34. doi:10.1186/cc2454
5. Balan V, Mihai C, Cojocaru F et al. Vibrational Spectroscopy Fingerprinting in Medicine: from Molecular to Clinical Practice. MDPI. https://www.mdpi.com/1996-1944/12/18/2884. Published 2020.
6. Atkins, C. G., Buckley, K., Blades, M. W., & Turner, R. F. (2017). Raman spectroscopy of blood and blood components. *Applied spectroscopy*, 71(5), 767-793.
7. Brunner, H., Sussner, H., Mayer, A. (1972). "Resonance raman scattering on the Haem group of oxy- and deoxyhaemoglobin." J. Mol. Biol. 70(1):153-156.
8. R.J. Stokes, E. McBride, C.G. Wilson, J.M. Girkin, W.E. Smith, D. Graham. ''Surface-Enhanced Raman Scattering Spectroscopy as a Sensitive and Selective Technique for the Detection of Folic Acid in Water and Human Serum''. Appl. Spectrosc. 2008. 62(4): 371–376.
9. Lemler P, Premasiri W, DelMonaco A, Ziegler L. NIR Raman spectra of whole human blood: effects of laser-induced and in vitro hemoglobin denaturation. Anal Bioanal Chem. 2013;406(1):193-200. doi:10.1007/s00216-013-7427-7
10. Berger, A. J., Koo, T. W., Itzkan, I., Horowitz, G., & Feld, M. S. (1999). Multicomponent blood analysis by near-infrared Raman spectroscopy. *Applied optics*, *38*(13), 2916-2926.
11. Lussier, F., Thibault, V., Charron, B., Wallace, G. & Masson, J. Deep learnging and artificial intelligence methods for Raman and surface-enhanced Raman scattering. *Trends in Analytical Chemistry* **124** (2020).
12. Haaland, D. & Thomas, E. Partial Least-Squares Methods for Spectral Analyses.1.Relation to Other Quantitative Calibration Methods and theExtraction of Qualitative Information. *Analytical Chemistry* **60**, 1193-1202 (1988).
13. Vigneau, E., Devaux, M., Qannari, E. & Robert, P. Principal component regression, ridge regression and ridge principal component regression in spectroscopy calibration. *Journal of Chemometrics* **11** (1998).

14. Balabin, R. & Lomankina, E. Support vector machine regression (SVR/LS-SVM)--an alternative to neural networks (ANN) for analytical chemistry? Comparison of nonlinear methods on near infrared (NIR) spectroscopy data. *Analyst* **136**, 1703-1712 (2011).
15. Martin MJ, Holcomb JB, Polk T, Hannon M, Eastridge B, Malik SZ, Blackman VS, Galante JM, Grabo D, Schreiber M, Gurney J, Butler FK, Shackelford S. The "Top 10" research and development priorities for battlefield surgical care: Results from the Committee on Surgical Combat Casualty Care research gap analysis. J Trauma Acute Care Surg. 2019 Jul;87(1S Suppl 1):S14-S21. doi: 10.1097/TA.0000000000002200. PMID: 31246901.
16. Rankin, I. A., Webster, C. E., Gibb, I., Clasper, J. C., & Masouros, S. D. (2020). Pelvic injury patterns in blast: Morbidity and mortality. *Journal of Trauma and Acute Care Surgery*, *88*(6), 832-838.
17. Unger, V., Grosse-Siestrup, C., Fehrenberg, C., Fischer, A., Meissler, M., & Groneberg, D. A. (2007). Reference values and physiological characterization of a specific isolated pig kidney perfusion model. *Journal of occupational medicine and toxicology (London, England)*, *2*, 1. https://doi.org/10.1186/1745-6673-2-1
18. Hofmaier, F., Dinger, K., Braun, R., & Sterner-Kock, A. (2013). Range of blood lactate values in farm pigs prior to experimental surgery. *Laboratory animals*, *47*(2), 130-132.
19. Harris, W. H. (1974). Hemoglobin, blood gases and serum electrolyte values in swine. *The Canadian Veterinary Journal*, *15*(10), 282.
20. Ally, A. (2019, August 09). Avoiding hemolysis in blood sample collection and processing. Insights Online Blog – Fisher Clinical Services. https://www.fisherclinicalservices.com/en/learning-center/insights-blog-overview/avoiding-hemolysis-in-blood-sample-collection-and-processing.html
21. Ki, K. K., Passmore, M. R., Chan, C., Malfertheiner, M. V., Fanning, J. P., Bouquet, M., Millar, J. E., Fraser, J. F., & Suen, J. Y. (2019). Low flow rate alters haemostatic parameters in an ex-vivo extracorporeal membrane oxygenation circuit. Intensive care medicine experimental, 7(1), 51. https://doi.org/10.1186/s40635-019-0264-z
22. Fried, J.A., Masoumi, A., Takeda, K. et al. How I approach weaning from venoarterial ECMO. Crit Care 24, 307 (2020). https://doi.org/10.1186/s13054-020-03010-5
23. Walter, J. M., Kurihara, C., Corbridge, T. C., & Bharat, A. (2018). Chugging in patients on veno-venous extracorporeal membrane oxygenation: An under-recognized driver of intravenous fluid administration in patients with acute respiratory distress syndrome?. Heart & lung : the journal of critical care, 47(4), 398–400. https://doi.org/10.1016/j.hrtlng.2018.03.011
24. Radiometer America (2011). ABL 800 BGA: Operators Manual. Brea, California: Author.
25. Radiometer America (2004). ABL 800 BGA: 510(k) Substantial Equivalence Determination Decision Summary. https://www.accessdata.fda.gov/cdrh_docs/reviews/K041874.pdf
26. Snaith, B., Harris, M. A., Shinkins, B., Jordaan, M., Messenger, M., & Lewington, A. (2018). Point-of-care creatinine testing for kidney function measurement prior to contrast-enhanced diagnostic imaging: evaluation of the performance of three systems for clinical utility. *Clinical Chemistry and Laboratory Medicine (CCLM)*, *56*(8), 1269-1276.
27. Suardi, N., Adelusi, S. M., & Terver, D. (2020). Therapeutic exposure of diabetic blood using 532 nm-wavelength low level laser through electrical impedance spectroscopy (EIS). Science Proceedings Series, 2(1), 98-104.

28. Premasiri, W. R., Lee, J. C., & Ziegler, L. D. (2012). Surface-enhanced Raman scattering of whole human blood, blood plasma, and red blood cells: cellular processes and bioanalytical sensing. *The Journal of Physical Chemistry B*, *116*(31), 9376-9386.
29. Zhao, J., Lui, H., McLean, D. I. & Zeng, H. Automated autofluorescence background subtraction algorithm for biomedical Raman spectroscopy. *Appl Spectrosc* **61**, 1225-1232, doi:10.1366/000370207782597003 (2007).

12.0 FIGURES AND TABLES:

Figure 1. A schematic drawing of the oxygenation and Raman measurement circuit used to collect data during this study.

Figure 2. Flow diagram depicting the multiple steps and feedback loops performed in "SpectralPreprocessing" to properly prepare the data to be fed into the machine learning algorithm.

Figure 3. A flow diagram displaying the overall process created by the code to generate machine learning algorithms (see text for a full description) and determine their root mean square error (RMSE) in fitting the dataset. The input is comma separated value (CSV) files and the output is R data serialized (RDS) files.

Figure 4. Fluorescence corrected Raman spectra of 3 L/min blood with a 15 second exposure.

Figure 5. Fluorescence and flow corrected Raman spectra of 3 L/min blood with a 15 second exposure.

Figure 6. Plots of the training and test data and resulting model for 15 seconds exposure time focusing on Creatinine at flow rates of 0 L/min (static), 1 L/min, and 3 L/min.

Table 1. Analyte concentration and pH targets for Creatinine (C), Glucose (G) and Lactic Acid (LA).

Table 2. Comparison of normal swine physiological levels for creatinine, glucose, lactic acid and pH and the range of observed values for each.

Table 3. The optimal signal processing methods and RMSE values for all analytes at each combination of flow rate and exposure time. PCR: Principle component regression; SVR-L: support vector regression, linear; SVR-R: support vector regression, Gaussian radial; PLS: partial least squares.

Table 4. RMSE values of all algorithms generated for each combination of flow rate, exposure time, and analyte using each of the 4 signal processing methods at padding = 125 and spline points = 35.

13.0 LIST OF SYMBOLS, ABBREVIATIONS AND ACRONYMS

AFB: Air Force Base
ApS: Anpartsselskab
AWS: Amazon Web Services
BGA: Blood gas analyzer
BLDG: Building
C: Creatinine

CARET : Classification and regression training
CSV: Comma separated value
DTIC: Defense Technical Information Center
ECMO: Extracorporeal membrane oxygenation
ELSO: Extracorporeal Life Support Organization
FDA: Food and Drug Administration
G: Glucose
GmbH: Gesellschaft mit beschränkter Haftung
JBSA: Joint Base San Antonio
LA: Lactic acid
LLC: Limited liability corporation
MD: Medical Doctor
NAMRU-SA: Navy Medical Research Unit, San Antonio
NIRS: Near-infrared spectroscopy
PBC: Public benefit corporation
PCR: Principal component regression
PhD: Doctor of Philosophy
PLS: Partial least squares
RBC: Red blood cells
RDS: R data serialized
RMSE: Root mean squared error
RN: Registered Nurse
RRS: Raman resonance spectroscopy
SVR-L: Support vector regression-linear
SVR-R: Support vector regression-Gaussian radial